

# Predicting the Acoustics of Arbitrarily Shaped Bodies Using an Integral Approach

William A. Bell,\* William L. Meyer,† and Ben T. Zinn‡  
*Georgia Institute of Technology, Atlanta, Ga.*

An integral solution of the Helmholtz equation is developed for predicting the acoustic properties of arbitrarily shaped bodies. With the integral formulation, the acoustic potentials at the surface are solved independently of the internal acoustic field which, effectively, reduces the dimensionality of the problem by one. Considerable reductions in computation time and storage requirements are thus achieved. Efficient numerical techniques for solving the resulting algebraic equations are presented. Numerical results obtained for the two-dimensional problems of a circle and a rectangle agree to within one percent with available exact solutions. The modes of a star-shaped configuration and a duct with a right-angle bend are also determined to demonstrate the applicability of this method to complicated geometries and general boundary conditions. The acoustic properties of a sphere are investigated using an axisymmetric formulation. With the axisymmetric formulation the numerical and exact results agree to three significant figures.

## I. Introduction

THE prediction of the acoustics of arbitrarily shaped bodies has a variety of applications in aerospace engineering. Among them are the determination of the internal and radiated sound fields from airbreathing propulsion systems and the investigation of the stability limits of rocket combustors. These studies are concerned with obtaining solutions to the Helmholtz equation, which is derived from the wave equation when a sinusoidal time dependence is assumed and which describes the spatial dependence of the oscillations. This equation is included in most standard texts on differential equations of mathematical physics (Ref. 1, Ch. 11) and has been extensively studied in both differential and integral form. The differential form is currently the most widely used.

In differential form, solutions of the Helmholtz equation can be obtained by separation of variables.<sup>1,2</sup> This method involves series expansions of the solutions in terms of eigenfunctions of the system. Although this technique has been successfully applied to several practical problems in duct wave propagation,<sup>3-9</sup> it has the following limitations: 1) the series expansions often involve special functions which are difficult to compute; 2) at high frequencies and at the boundaries the series are slowly convergent—therefore, a large number of terms in the series must be retained to ensure accurate results, which often requires excessive computation time; 3) this method can only be used with special coordinate systems and boundary conditions for which the separation of variables can be applied. At present only eleven suitable coordinate systems are known (Ref. 1, p. 513ff).

For arbitrarily shaped bodies, the differential form of the Helmholtz equation can be solved by writing the equation in terms of finite differences (Ref. 1, p. 703ff). Unlike separation of variables, this technique is not limited to ducts with simple geometries. A typical application of finite differences is given by Wynne and Plumlee<sup>10</sup> who solved for the transverse eigenvalues and eigenfunctions of an annular duct with lined walls. This technique involves the simultaneous solution of the acoustic potential value at every point within the duct. Once the potential values are known,

the acoustic pressure and velocity can then be determined. To obtain sufficient accuracy, fine grid sizes must be used which necessitates large computer storage requirements. This drawback was noted by Baumeister,<sup>11</sup> Baumeister and Rice,<sup>12</sup> and Alfredson<sup>13</sup> who used this technique in studies of duct wave propagation. Because of the storage requirements this technique has mainly been applied to two-dimensional problems. For three-dimensional problems numerical methods capable of handling large matrices must be used which require considerable computer time and computational effort.<sup>14</sup> This technique is also impractical in radiation problems which involve infinite domains.

To avoid the limitations of the differential formulation, the integral approach is employed in this study. The integral approach has been successfully applied to a wide range of acoustic problems. In determining the sound radiation field from vibrating surfaces, integral techniques have been widely used.<sup>15-18</sup> For example, Chen and Schweikert<sup>15-16</sup> employed this method to determine the radiation sound patterns for three-dimensional shapes with mixed boundary conditions. To check the accuracy of the results, they computed the radiated field produced by a piston vibrating on a sphere. For this problem an exact solution exists<sup>3</sup> and compares favorably with the numerical results. The integral formulation is also used to solve the problem of scattering by arbitrary shapes.<sup>15-21</sup> Banaugh and Goldsmith, for example, used this technique to investigate the effect of surface shape<sup>19</sup> on scattered sound fields. By applying this method to a circular cylinder, for which exact solutions are available,<sup>3,4</sup> and comparing the exact and numerical solutions, Banaugh and Goldsmith demonstrated the accuracy of the integral solution scheme. Although this method is capable of handling mixed boundary conditions, only surfaces with rigid boundaries were considered in Ref. 19. The effect of mixed boundary conditions was included in studies by Liu and Martenson<sup>22</sup> and Quinn<sup>23</sup> of the internal acoustic pattern of lined ducts with arbitrary shapes. Comparison of the theoretical predictions with experimental data showed generally good agreement. Unpublished work by Zinn and Gaylord<sup>24</sup> demonstrated the applicability of the integral formulation for the determination of the natural frequencies and modes for two-dimensional shapes. In this study the accuracy of the technique was determined by comparing the natural frequencies and mode shapes with available exact solutions for a two-dimensional cylinder with rigid walls. The agreement is to within four decimal places which is two-orders-of-magnitude more accurate than previous results

Presented as Paper 76-494 at the 3rd AIAA Aero-Acoustics Conference, Palo Alto, Calif., July 20-23, 1976; submitted Aug. 2, 1976; revision received March 15, 1977.

Index categories: Noise; Aeroacoustics.

\*Instructor. Member AIAA.

†Research Associate.

‡Regents' Professor. Associate Fellow AIAA.

obtained by solving the differential Helmholtz equations using finite differences.<sup>10</sup> In another study by Tai and Shaw,<sup>25</sup> the integral method was applied to a right triangle. The resulting eigenfrequencies compared with exact solutions to within 5% and the maximum deviation between the numerically computed and exact potential fields was less than 1%.

To demonstrate the accuracy and the versatility of the integral solution technique, results are obtained for several acoustic problems involving a variety of geometries. To obtain a solution, the integral equation is first discretized to form a system of algebraic equations which are then solved for the acoustic potential at discrete points on the boundary. From these values the rest of the sound field is obtained. Methods for increasing the numerical accuracy by use of Gaussian quadrature and other numerical integration methods are presented and discussed. The first problem considered is the numerical evaluation of the resonant frequencies and natural modes of two-dimensional circular, rectangular, and star configurations. Exact and numerical values are compared for the circle and rectangle. The next problem considered is a two-dimensional duct with a right-angle bend with a sound source at one end and sound absorption treatment at various locations along the duct. The results are compared with finite difference solutions. These studies demonstrate the applicability of the integral formulation to complicated geometries and general boundary conditions. The next problem considered is the two-dimensional radiation problem of a piston set in a right circular cylinder. Again, the exact and numerical acoustic fields are computed and compared. Finally, a three-dimensional problem of determining the acoustic properties of a sphere is considered. The internal field is obtained using an axisymmetric formulation.

## II. Governing Equations

The integral formulations of the wave equation for internal and radiation acoustic problems are developed in this section for two and three dimensions. The boundary conditions generally encountered in practical problems are then discussed. For clarity, only a brief account of the derivation of the basic equations will be given in this section. For a more detailed and rigorous development, Refs. 26 through 29 can be consulted.

Assume a frictionless, homogeneous gas, and let  $\rho_0$  and  $p_0$  be the density and pressure of the fluid at rest. Representing the acoustic pressure and particle velocity at a time  $t$  by  $p$  and  $u$ , Euler's equation for the conservation of momentum gives

$$\rho_0 \frac{\partial u}{\partial t} + \nabla p = 0 \quad (1)$$

The continuity equation yields the relationship

$$\frac{\partial p}{\partial t} + \rho_0 c_0^2 \nabla \cdot u = 0 \quad (2)$$

where  $c_0$  is the speed of sound. By defining an acoustic potential function  $\Psi$  such that

$$u = \nabla \Psi \quad (3)$$

Equation (1) provides the relation

$$p = -\rho_0 \frac{\partial \Psi}{\partial t} \quad (4)$$

and Eq. (2) results in the classical wave equation

$$\nabla^2 \Psi - \frac{1}{c_0^2} \frac{\partial^2 \Psi}{\partial t^2} = 0 \quad (5)$$

The wave equation can also be written in terms of  $p$  and  $u$ , but it is more convenient to work with an acoustic potential function, from which both the acoustic pressure and particle velocity can readily be obtained.

Equation (5) is the wave equation for a general time dependence and can be written in integral form and solved by using retarded potentials.<sup>21,28</sup> However, for most practical problems a sinusoidal time dependence can be assumed which simplifies the problem considerably. Assume

$$\Psi(r, t) = \phi(r) e^{i\omega t} \quad (6)$$

Substituting Eq. (6) into Eq. (5) gives the Helmholtz equation

$$\nabla^2 \phi + k^2 \phi = 0 \quad (k = \omega/c_0) \quad (7)$$

which can be solved by simpler methods not involving the use of retarded potentials.

### Integral Formulation

To obtain an integral formulation of the Helmholtz equation, consider the problem shown in Fig. 1. Applying Green's theorem to the Helmholtz equation<sup>1,28,29</sup> gives the following integral relation

$$\int_{\Gamma} \left[ \phi(Q) \frac{\partial G(P, Q)}{\partial n_Q} - G(P, Q) \frac{\partial \phi(Q)}{\partial n_Q} \right] dS_Q = 0 \quad (8)$$

where  $\phi$  is the acoustic potential function and  $G$  is the Green's function defined by Eqs. (14-16), which also satisfies the Helmholtz equation. The Green's function is regular inside the surface except when  $P=Q$ . At this point  $G$  is singular. To remove this singularity from the integral given by Eq. (8), point  $P$  is surrounded by a small sphere or circle  $\sigma$  of radius  $\epsilon$ . The integral will now include a term over  $\sigma$  which, on taking the limit as  $\epsilon \rightarrow 0$ , gives

$$\phi(P) = C \int_{\Gamma} \left[ G(P, Q) \frac{\partial \phi(Q)}{\partial n_Q} - \phi(Q) \frac{\partial G(P, Q)}{\partial n_Q} \right] dS_Q \quad (9)$$

where  $C$  is  $i/4$  for two dimensions and  $1/4\pi$  for axisymmetric and three-dimensional shapes.

From Eq. (9) the value of the acoustic potential function at any point  $P$  within the surface can be determined from the boundary values of the potential and its normal derivative. Thus, the entire wave pattern within the surface can be constructed. For arbitrarily shaped surfaces for which numerical techniques must be used to obtain a solution, Eq. (9) requires much less computer storage than the differential

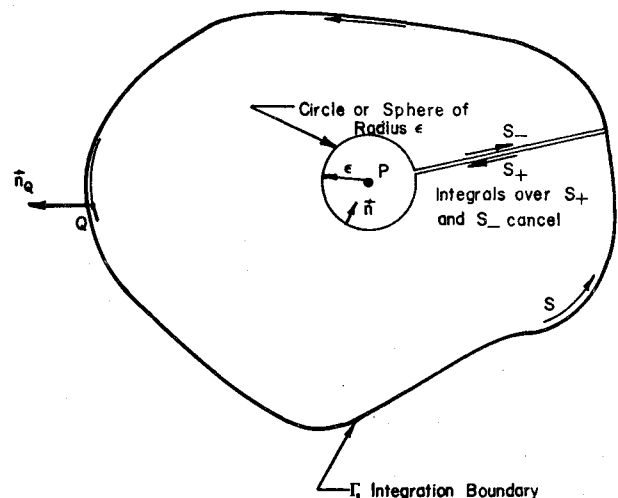


Fig. 1 Integration surface for an interior point.

formulation given by Eq. (7). Using Eq. (9) the value of the potential at each interior point can be obtained independently, whereas the method of finite differences used to solve Eq. (7) requires the simultaneous solution of  $\phi$  for every interior point. The integral formulation avoids the large matrices involved with finite differences.

If the values of both  $\phi$  and  $\partial\phi/\partial n$  are known at every point on the boundary then the wave pattern can readily be determined from Eq. (9). However, for most practical acoustic problems either  $\partial\phi/\partial n$  or an admittance condition relating  $\phi$  and  $\partial\phi/\partial n$  are given. Therefore, the values of the acoustic potential at the boundary must first be determined. The necessary relation is obtained by letting the point  $T$  approach the boundary at some point  $Q$  to obtain the following relation<sup>26</sup>

$$\phi(T) = 2C \int_{\Gamma} [G(T, Q) \frac{\partial\phi(Q)}{\partial n_Q} - \phi(Q) \frac{\partial G(T, Q)}{\partial n_Q}] dS_Q \quad (10)$$

Eq. (10) is applicable to a smooth boundary, but has been extended to include cusps and corners.<sup>19,24</sup> To obtain the interior wave pattern, Eq. (10) is first solved for the boundary values of  $\phi$ . These values are then substituted into Eq. (9) to determine the acoustic potential at the interior points. Both Eqs. (9) and (10) involve singular integrands as  $T$  approaches  $Q$  although for smooth surfaces the integrals themselves are regular.

For exterior problems, analogous expressions to Eqs. (9) and (10) are obtained by taking the point  $P$  outside the surface  $\Gamma$ .<sup>4</sup> The integration in Eq. (8) is then carried out over the boundary, around a circle or sphere of radius  $\epsilon$  with point  $P$  as a center, and then around a circle or sphere of radius  $R$ , which is arbitrarily large. In this manner the integration includes the entire external domain. However, by applying Sommerfeld's radiation condition, it can be shown that the integral about the infinite sphere or circle approaches zero as  $R$  approaches infinity.<sup>4</sup> Thus, the corresponding equations for the external domain become

$$\phi(P) = -C \int_{\Gamma} [G(P, Q) \frac{\partial\phi(Q)}{\partial n_Q} - \phi(Q) \frac{\partial G(P, Q)}{\partial n_Q}] dS_Q \quad (11)$$

and

$$\phi(T) = -2C \int_{\Gamma} [G(T, Q) \frac{\partial\phi(Q)}{\partial n_Q} - \phi(Q) \frac{\partial G(T, Q)}{\partial n_Q}] dS_Q \quad (12)$$

It is important to note that Eqs. (11) and (12) involve integrations about the boundary of the body only. Thus, the radiated field at any distance from the body can be obtained once the surface acoustic potential is known. With finite differences, the values of the potential at every point in a very large domain would have to be computed in order to obtain the radiated field. Also, an artificial boundary condition at a large distance from the surface must be assumed. These factors make the application of finite differences to problems of this type rather inefficient whereas the integral formulation can readily be adopted to such situations.

Eqs. (9) through (12) are applicable to two-dimensional, axisymmetric, and three-dimensional acoustic problems. In the two-dimensional and axisymmetric cases, these equations involve line integrals; and in the three-dimensional case, the integrals are taken over a surface. Note that the dimensionality of the problem is reduced by one—a valuable simplification.

The Green's functions satisfy the following inhomogeneous forms of the Helmholtz reduction with homogeneous boundary conditions<sup>1</sup>

$$\nabla^2 G + k^2 G = \delta(P - Q) \quad (13)$$

where  $\delta$  is the Dirac delta function. The Green's functions are<sup>1,17,18</sup>

$$G(P, Q) = H_0^{(1)}(kr) \text{ for two dimensions,} \quad (14)$$

$$G(P, Q) = 2 \int_0^\pi \frac{e^{ikr}}{r} \cos m\theta d\theta \text{ for axisymmetric bodies} \quad (15)$$

and

$$G(P, Q) = e^{-ikr}/r \text{ for three dimensions} \quad (16)$$

where  $r$  is the distance between points  $P$  and  $Q$ , and  $H_0^{(1)}(kr)$  is the zeroth order Hankel function of the first kind.

**Boundary Conditions**

The two most common boundary conditions in practical acoustic problems are the Neumann and Robin conditions. The Neumann condition of interest in the present study is

$$\partial\phi/\partial n = A \quad (17)$$

where  $A$  is the velocity amplitude of a given sound source. In the absence of a sound source  $A = 0$ ; this condition means that the particle velocity is zero at the boundary which implies a perfectly reflecting, or rigid surface. For surfaces which absorb sound, such as lined duct walls, an admittance condition is usually specified, which leads to the Robin condition. Defined as the ratio of the normal component of the particle velocity to the pressure perturbation, the admittance  $y$  can be written as

$$y = \rho_0 c_0 (u_n/p) \quad (18)$$

Substituting for  $u_n$  and  $p$  from Eqs. (3) and (4) gives

$$(\partial\phi/\partial n) + ik y \phi = 0 \quad (19)$$

Eq. (19) is the Robin condition.<sup>29</sup> For sound-absorbing materials or devices, the admittance can be either analytically determined<sup>30-32</sup> or measured using the impedance tube or a related technique.<sup>33-34</sup> The effects of a given material on the internal acoustic properties of a particular geometry can be

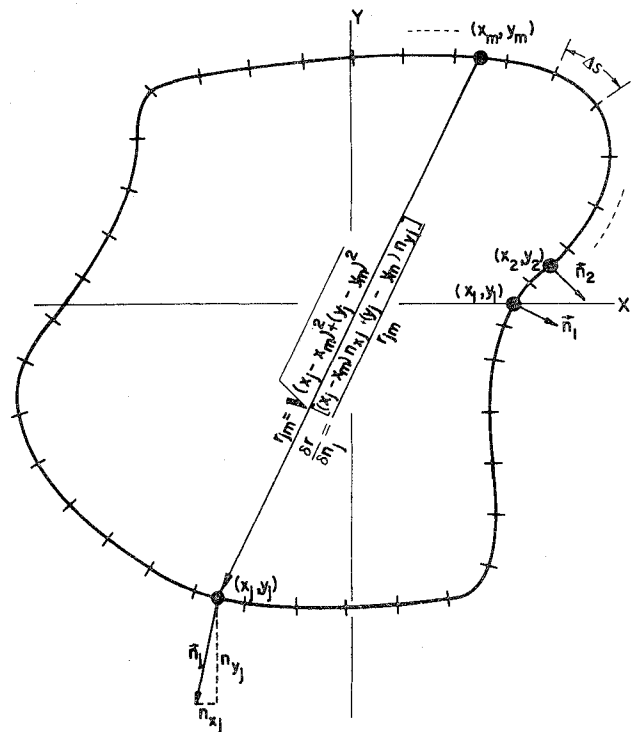


Fig. 2 Geometric considerations for the general problem.

determined by substituting the admittance of the material into Eq. (19) and solving Eqs. (9) and (10) or (11) and (12) for the acoustic potential. Thus, the analytical techniques used in this investigation is applicable to a vast number of duct acoustic problems. Since the admittance of a combustion process can also be measured,<sup>35</sup> this analysis can also be applied to related linear combustion instability problems, provided that the equations are applied to regions where the Helmholtz equation holds and mean flow effects can be neglected. By replacing the combustion process by an admittance condition, studies of combustion instability have been conducted in liquid and solid propellant combustors.<sup>36-37</sup> This research allows the extension of these analyses to more general shapes.

Substituting Eq. (19) into Eq. (10) gives for the internal field

$$\begin{aligned} \phi(T) + 2C \int_{\Gamma} \phi(Q) \left[ \frac{\partial G(T, Q)}{\partial n_Q} + iky(Q)G(T, Q) \right] dS_Q \\ = -2C \int_{\Gamma} A(Q)G(T, Q) dS_Q \end{aligned} \quad (20)$$

A similar expression is obtained from Eq. (12) for the exterior problem. For surfaces with spatially varying admittances, the admittance is a function of  $Q$ . For most cases considered in this study,  $y$  is assumed constant although nonuniform admittance distributions can be easily handled.

### III. Solution Technique

In the last section, the integral equations were developed which describe the interior and exterior acoustic fields or a surface with arbitrary shape and mixed boundary conditions. The numerical solution technique for solving these equations to obtain the internal or radiated acoustic patterns is presented in this section and can be divided into four parts. The first is the discretization of the integral equations into a corresponding system of linear, and algebraic equations in  $\phi$  suitable for solution on a computer. The second part is the specification of the geometry and boundary conditions. The third is the computation of the coefficients of the system of equations and the final part is the methods used to solve for the surface potential from the algebraic equations.

#### Discretization of the Integral Equations

In two dimensions and for axisymmetric problems, Eq. (20) involves a one-dimensional improper integral about the boundary line. For this type of problem several numerical integration techniques<sup>38-39</sup> are available. The simplest is the trapezoidal rule which has been shown to yield excellent results in two-dimensional studies with this type of integral.<sup>19,24,25</sup> Using this numerical integration scheme, Eq. (20) becomes

$$\begin{aligned} \phi_m + 2C \sum_{j=1}^N \phi_j \left[ \frac{\partial G(r_{jm})}{\partial n_j} + iky_j G(r_{jm}) \right] \Delta S_j \\ = -2C \sum_{j=1}^N A_j G(r_{jm}) \Delta S_j \end{aligned} \quad (21)$$

where one equation for  $\phi$  is obtained for each value of  $m$  and  $m$  is varied from 1 to  $N$ . Eq. (21) was initially used in this investigation to generate the  $N$  equations for  $\phi$  and accurate results were obtained when the admittance  $y$  was zero everywhere on the boundary<sup>40</sup> which is the case considered in previous studies.<sup>19,24,25</sup> However, when a nonzero admittance is assumed, this technique gives inaccurate results because of the contribution from the Green's function when the point  $j$  approaches  $m$ . Because of the singular nature of the Green's function at the point  $m$ , care must be taken when numerically integrating this function over the subinterval  $m$ . To increase the accuracy in evaluating the integrand, Eq. (20) is broken up into  $N$  integrals given by Eq. (22).

$$\begin{aligned} \phi_m \left\{ 1 + 2C \int_{S_{m-1/2}}^{S_{m+1/2}} \left[ \frac{\partial G(r_{1/2})}{\partial n_{1/2}} + iky_m G(r_{1/2}) \right] dS_j \right\} \\ + 2C \sum_{\substack{j=1 \\ j \neq m}}^N \phi_j \int_{S_{j-1/2}}^{S_{j+1/2}} \left[ \frac{\partial G(r_{jm})}{\partial n_j} + iky_j G(r_{jm}) \right] dS_j \\ = -2C \sum_{j=1}^N A_j \int_{S_{j-1/2}}^{S_{j+1/2}} G(r_{jm}) dS_j \end{aligned} \quad (22)$$

In both Eqs. (21) and (22) the values of  $\phi$  are assumed to be constant over each of the  $N$  subintervals. The difference is the method by which the terms involving the Green's function are evaluated. In Eq. (21) an average value is computed over each of the subintervals based on  $r_{jm}$ . With Eq. (22) these terms are integrated numerically from  $r_{j-1/2,m}$  to  $r_{j+1/2,m}$  using Gaussian quadrature<sup>39-40</sup> to obtain more accurate values. This type of formulation has been used before with trapezoidal instead of Gaussian quadrature formulas.<sup>18</sup> In the present study for two-dimensional and axisymmetric problems, a reduction in error of two orders of magnitude in the numerical results for a nonzero admittance was achieved using Eq. (22) instead of Eq. (21).<sup>40</sup>

#### Surface Geometry and Boundary Conditions

The first step in solving Eq. (22) is the determination of the coefficients of  $\phi_j$  and  $\phi_m$ . These coefficients depend upon the surface geometry through the terms  $\partial/\partial n_j$ ,  $r_{jm}$ , and  $\Delta S_j$ . By specifying the admittance  $y$  and/or the sound velocity amplitude  $A$  over every subinterval  $j$ , the effect of the boundary conditions are included in the evaluation of the coefficients.

To solve for the terms involving the surface geometry, the first expression inside the integrals of Eq. (22) is written as

$$\frac{\partial G(r)}{\partial n} = \frac{\partial G(r)}{\partial r} \frac{\partial r}{\partial n}$$

Th expressions for  $\partial G/\partial r$  are obtained by differentiating Eqs. (14) through (16). Substituting this expression into Eq. (22)

Table 1 Eigenfrequencies and natural modes of a circle for various admittance values

MODE		ADMITTANCE VALUE		
		y = 0 <sup>a</sup>	y = 0.3	y = 0.3i <sup>c</sup>
	COMPUTED	1.84122	1.8324+0.4423i	1.4441-0.0071i
	EXACT	1.84118	1.8322+0.4432i	1.4384
	COMPUTED	3.05423	3.0791+0.5397i	2.5369-0.0151i
	EXACT	3.05424	3.0786+0.5442i	2.5427
	COMPUTED	3.83175	Not Computed	Not Computed
	EXACT	3.83171	3.8188+0.3095i	3.5510
	COMPUTED	4.20135	4.2538 0.6199i	3.5816 - 0.0231i
	EXACT	4.20119	4.2532 0.6351i	3.5615
	COMPUTED	5.31783	Not Computed	Not Computed
	EXACT	5.31755	5.3953 0.7101i	4.5767

Table 2 Resonant frequencies and natural modes of a rectangle for different admittance values at the ends

MODE		ADMITTANCE VALUE		
		y = 0	y = 0.3	y = 0.3i
	COMPUTED	3.1432	3.150 + 0.6199i	2.558 + 0.0021i
	EXACT	3.1416	3.142 + 0.6190i	2.559
	COMPUTED	6.2877	6.302 + 0.6156i	5.886 + 0.0021i
	EXACT	6.2832	6.283 + 0.6190i	5.884
	COMPUTED	7.0312	7.146 + 0.5881i	6.333 - 0.007i
	EXACT	7.0248	Not Computed	6.283
	COMPUTED	8.893	8.934 + 0.6101i	8.303 - 0.011i
	EXACT	8.886	Not Computed	8.299
	COMPUTED	9.4329	9.456 + 0.6106i	8.847 + 0.0071i
	EXACT	9.4248	9.425 + 0.6190i	8.842i

gives a relation which involves  $\partial r/\partial n_j$ ,  $r_{jm}$  and  $dS$ . The expressions for  $\partial r/\partial n_j$ ,  $r_{jm}$  and  $dS$  can be written in parametric form for bodies with simple shapes, and this type of representation has been used in previous studies using simple geometries.<sup>19-20,24,41,42</sup> By taking advantage of symmetry, considerable savings in computer storage and computation times were achieved. In fact, Greenspan and Werner<sup>42</sup> showed that for a circle, Eq. (22) can be reduced to a single equation instead of a system of equations which could readily be solved to obtain the acoustic field. In the study by Tai and Shaw,<sup>25</sup> the method of images (Ref. 1, Ch. 11) was used to greatly reduce the number of points necessary to compute eigenfrequencies and eigenmodes of a family of triangles. Although these studies demonstrate valuable simplifications which can be made in applying the integral formulation to a particular problem, the techniques used are not applicable to more general problems involving complicated geometries and nonuniform boundary conditions.

In the present study for two dimensions, the expressions for the geometric variables are written in parametric form only for the circle. In the rest of the configurations considered, a general formulation is used. The fact that a parametric representation cannot be used in general cases is not a serious drawback—in fact, it somewhat simplifies the formulation. Consider the general two-dimensional problem depicted in Fig. 2. By specifying the  $x$  and  $y$  coordinates at the midpoint of each of the subintervals, the distance  $r_{jm}$  is readily computed from the expression

$$r_{jm} = \sqrt{(x_j - x_m)^2 + (y_j - y_m)^2} \quad (23)$$

The expression for  $\partial r/\partial n_j$  can then be obtained since it represents the dot product of the gradient of  $r$  and the normal at  $j$ . Thus,

$$\frac{\partial r}{\partial n_j} = \frac{(x_j - x_m)n_{xj} + (y_j - y_m)n_{yj}}{r_{jm}} \quad (24)$$

where  $n_{xj}$  is the component of the normal vector  $j$  in the  $x$  direction (or the cosine of the angle between the normal vector and the  $x$ -axis) and  $n_{yj}$  is the corresponding  $y$  component (the sine of the angle between the normal vector and the  $y$ -axis). Analogous expressions for  $r_{jm}$  and  $\partial r/\partial n_j$  can be obtained for axisymmetric<sup>17-18</sup> and three-dimensional problems. For two-dimensional and axisymmetric problems, the line segment length  $\Delta S_j$  is simply

$$\Delta S_j = \sqrt{(x_{j+1/2} - x_{j-1/2})^2 + (y_{j+1/2} - y_{j-1/2})^2}$$

or, for  $N$  equally spaced subintervals,  $S_j = L/N$  where  $L$  is the length of the perimeter of the surface. For three-dimensional bodies,  $\Delta S_j$  is the area of each of the subsurfaces taken over the boundary.

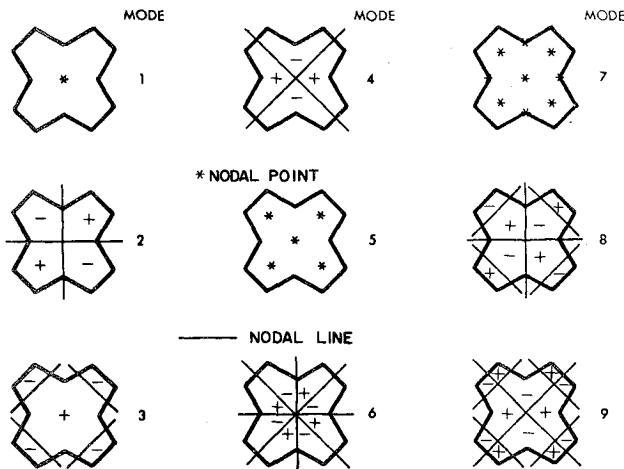


Fig. 3 Nodal points and lines for the first nine modes of the star.

**Computation of the Coefficients of the Discretized Integral Equation**

Once the geometry has been specified, the coefficient of  $\phi$  in Eq. (22) can be determined by evaluating the Green's functions  $G(r_{jm})$  and  $\partial G(r_{jm})/\partial r_{jm}$ . There are two problems in determining these functions: the first is a rapid, accurate method for computing them over a wide range of the argument  $kr_{jm}$ ; and the second is the singularity associated with each function as  $r_{jm}$  approaches zero.

For the two-dimensional problems to compute the Hankel functions two routines have been used in this study. The first consists of a series expansion using standard formulas for the Hankel function with complex arguments.<sup>39,43</sup> A sufficient number of terms is taken to satisfy a specified degree of accuracy. To minimize time, a different series expansion which was developed by Hitchcock<sup>44</sup> is used for determining these functions in the studies of the rectangle, star, and duct with a right-angle bend. With his formulation, accuracies of  $10^{-10}$  or greater are achieved using nine terms or less in the series expansion. Reductions of up to 50% in computer times can be achieved with this formulation.

For the axisymmetric problem, the integral in Eq. (15) is carried out using a 20-point Gauss-Legendre quadrature formula. For three-dimensional problems, evaluation of the Green's function given by Eq. (16) is straightforward.

The major problem in accurately computing the coefficients in Eq. (22) is the singularity associated with the Green's functions as  $r_{jm}$  approaches zero; that is, as the point  $j$  approaches  $m$  in Fig. 2. The two-dimensional and axisymmetric Green's functions have logarithmic singularities. In this study, the inaccuracies involved are minimized by subdividing the intervals as indicated by Eq. (22).

**Determination of the Acoustic Potential**

Once the coefficients of the surface potential at each discrete point on the surface are determined, the equations are solved for  $\phi$  using a complex Gauss-Jordan reduction scheme. The interior or exterior points can then be found using the discretized form of Eq. (9).

To determine the eigenfrequencies of a particular geometry, the technique described in Ref. 40 is used. Essentially, this technique consists of: 1) determining the frequency  $k$  for which the determinant of the coefficients in the homogeneous form of Eq. (22) is zero, 2) normalizing the equation at the eigenfrequency to obtain the surface distribution of the mode, and 3) using Eq. (9) in discretized form to find the interior sound field.

**V. Results**

Using the numerical techniques described in the last section, solutions have been obtained for a variety of two-dimensional and axisymmetric problems to demonstrate its broad range of

Table 3 Surface potentials for a circle of unit radius, second mode,  $Y = 0$

Angle	Numerical	Exact
12	.9130	.9135
24	.6681	.6691
36	.3077	.3090
48	-.1059	-.1045
60	-.5012	-.5000
72	-.8099	-.8090
84	-.9785	-.9781
96	-.9779	-.9781
108	-.8082	-.8090
120	-.4988	-.5000
132	-.1013	-.1045
144	.3104	.3090
156	.6702	.6691
168	.9141	.9135
180	1.0000	1.0000

**Table 4** Surface potential for a rectangle, height to width ratio = 0.5, first mode, rigid walls

	Y	Numerical	Exact
1/2	1/14	1.0061	1.0063
1/2	2/14	1.0060	1.0063
1/2	3/14	1.0055	1.0063
13/28	1/4	1.0000	1.0000
11/28	1/4	.9501	.9499
9/28	1/4	.8524	.8521
7/28	1/4	.7119	.7116
5/28	1/4	.5356	.5354
3/28	1/4	.3325	.3324
1/28	1/4	.1127	.1127

applications. The two-dimensional form of the integral equation has been used to compute the resonant frequencies and natural modes of a circle, rectangle, and star configuration. In addition, the problem of a duct with a right angle bend is considered, and results using Eq. (22) are compared with finite difference solutions. The two-dimensional problem of sound radiation from a right circular cylinder is then considered and the numerical and exact solutions are compared. Finally the acoustic properties of a sphere are computed using the axisymmetric formulation.

For a circle and rectangle, comparisons between exact and numerical solutions are presented in Tables 1 and 2. In these tables the numerical and exact eigenfrequencies are tabulated for three admittance values,  $y=0$ ,  $y=0.3$ ,  $y=0.3i$ , with thirty points taken on the boundary. The best agreement between the computed and exact results occurs at the zero admittance condition. For the circle, the real part of the eigenfrequencies compare to five significant figures and the imaginary parts are accurate to 0.001 for the first five modes. When a nonzero admittance condition is introduced, the accuracy is reduced to three significant figures in the real part and to 0.01 in the imaginary part of the eigenfrequencies.

As with the circle, the agreement between the exact and numerical values for the rectangle is good for a rigid boundary but deteriorates when a nonzero admittance is introduced. From Table 2 the agreement is to almost four significant figures in the real part of the eigenfrequency and to within 0.01 in the imaginary part for a rigid wall. The Gaussian integration techniques developed in Sec. III improve

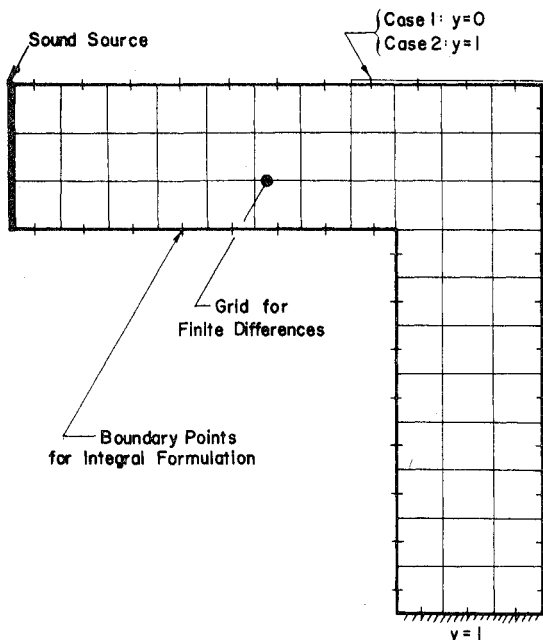


**Fig. 4** Locations of the discrete points, nonzero admittance boundaries, and the sound source for the duct with a right-angle bend.

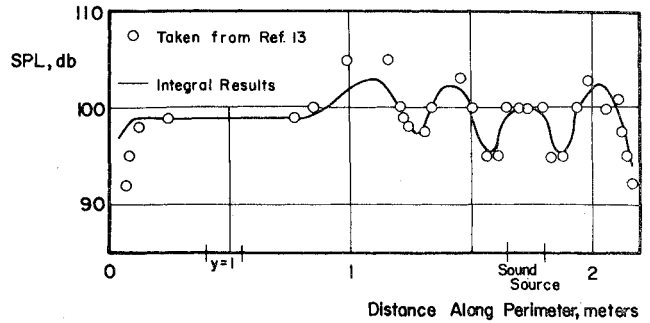


**Fig. 5** Comparison of numerical results for a duct with a right-angle bend using the integral and finite difference approaches, Case 1.

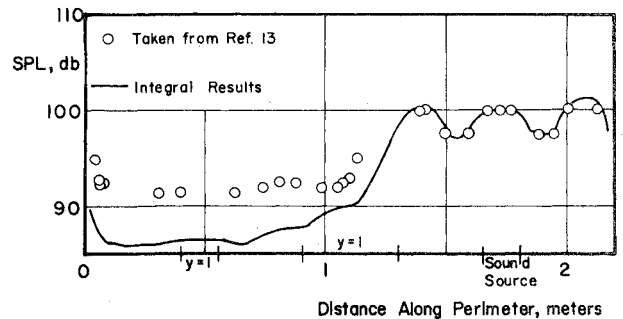


**Fig. 6** Comparison of numerical results for a duct with a right-angle bend using the integral and finite difference approaches, Case 2.

the accuracy of the computed eigenfrequencies for a nonzero admittance condition by an order of magnitude.

For the circle the accuracy of the computed natural mode shapes is shown in Table 3. The agreement between the exact and computed eigenmodes for a rigid boundary is to within 0.01% for interior points sufficiently far removed from the boundary. For a nonzero admittance at the surface, the accuracy is to within 2%. These results are obtained using the interior analog of Eq. (21) which explains the deterioration in accuracy of the interior points as the boundary is approached. Equation (22) is used in the studies of the rectangle, star, and duct problems and more accurate results are obtained close to the boundary. For the rectangle, the boundary values of the acoustic potential are presented in Table 4. The agreement between the exact and numerical results is within one-half of a percent. Computation times range from ten sec per eigenfrequency for the circle to 45 sec for the rectangle on UNIVAC 1108 computer. Using the discretized form of Eq. (9), interior points require approximately two sec per point to compute.

In studying the star-shaped boundary, which is of interest in solid-rocket combustion instability problems, the applicability of the integral solution technique to a complicated geometry for which separation of variables does not apply can be assessed. The first nine eigenfrequencies and natural modes for the star are presented in Fig. 3 for a rigid wall with 48 points taken on the surface. The most unique feature of the acoustic field for the star is the appearance of nodal points at some of the resonant modes. In the circle and rectangle nodal lines only are present, and they follow one of the separable coordinates of the boundary. With the star both nodal lines and points can occur which is in qualitative agreement with experimental observations for unstable solid propellant combustors. Computation times are from 60 to 75 sec per mode. The modes of a typical solid propellant configuration during a burn have also been computed and are given in Ref. 45.

The last internal two-dimensional problem investigated is that of a duct with a right-angle bend shown in Fig. 4. The reasons for studying this configuration are: 1) to investigate a

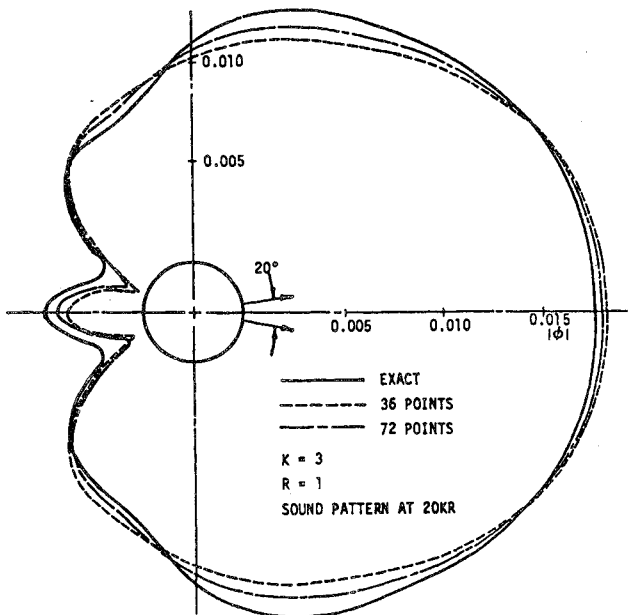


Fig. 7 Sound pattern produced by a 20° vibrating piston set in a circular cylinder.

nonuniform surface admittance, 2) to include a sound source in the integral formulation, and 3) compare the results obtained by the integral technique with the finite difference solutions of Ref. 13.

The results obtained using this configuration are presented in Figs. 5 and 6 and are compared with the solutions obtained using the finite difference method. Although the results using the integral approach are in qualitative agreement with the finite difference solution, quantitative agreement is lacking. The same number of boundary points are taken in both cases. Doubling the number of subintervals using Eq. (22) does not improve the agreement between the two sets of data. However, it does show that the results of the integral formulation are self-consistent. An experimental setup is

Table 5 Resonant frequencies and surface potentials for a sphere of unit radius, first and second modes, axisymmetric formulation

Resonant frequencies		
Computed		Exact
2.084-0.0041		2.082
3.346-0.0071		3.342
Normalized surface potential		
Angle	Computed	Exact
(First mode)		
5	1.00000	1.00000
15	.96960	.96962
25	.90975	.90977
35	.82232	.82228
45	.70992	.70981
55	.57593	.57577
65	.42439	.42423
75	.25992	.25981
85	.08753	.08749
(Second mode)		
5	1.0000	1.0000
15	.9098	.9099
25	.7403	.7405
35	.5121	.5124
45	.2275	.2529
55	-.0072	-.0066
65	-.2346	-.2348
75	-.4051	-.4041
85	-.4953	-.4942

<sup>a</sup>Numerical results obtained using Eq. (21) instead of Eq. (22).

currently being developed to check these results and should clarify the discrepancy between these two methods.

For two-dimensional radiation problems, excellent results are obtained as shown in Fig. 7. Here the radiated field from a piston set in a right circular cylinder is computed and compared with exact results from Ref. 3. The mean square error is less than 2% while the computation time required is 15 sec to obtain both the surface and far field patterns.

To check the accuracy of the axisymmetric formulation, the first two resonant frequencies and natural mode shapes of a sphere were computed and are presented in Table 5. As with the two-dimensional problems, agreement between the exact and numerical calculations is excellent. Computation times are approximately two minutes per mode; however, no attempt was made to take advantage of the symmetry of the problem which can reduce the computation time by at least a factor of two.

### Conclusions and Recommendations

The results for the circle and rectangle show that the integral technique is very accurate in determining resonant frequencies and natural mode shapes. Its application to the star configuration demonstrates its usefulness in studying the acoustics of complicated shapes. For the duct with a right-angle bend, the integral approach is shown to be applicable to nonuniform boundary conditions involving sound sources. The formulation also gives accurate results for two-dimensional radiation problems shown in the study of the right circular cylinder.

With the axisymmetric formulation accurate results are obtained for the internal eigenmodes of a sphere. Extensions to more complicated boundaries can readily be made.

### Acknowledgment

Most of this work was conducted under NSF Research Initiation Grant GK-42159.

### References

- <sup>1</sup>Morse, P. M. and Feshbach, H., *Methods of Theoretical Physics, Parts I and II*, McGraw-Hill, New York, 1953.
- <sup>2</sup>Weinberger, H. F., *A First Course in Partial Differential Equations*, Blaisdell, Waltham, Mass., 1965.
- <sup>3</sup>Morse, P. M. and Ingard, K. U., Ch. 9, *Theoretical Acoustics*, McGraw-Hill, New York, 1969.
- <sup>4</sup>Skudrzyk, E., *The Foundations of Acoustics*, Springer-Verlag, Vienna, Austria, 1971, Ch. 22 and 23.
- <sup>5</sup>Mitchell, C. E., Espander, W. R., and Baer, M. R., "Determination of Decay Coefficients for Combustors with Acoustic Absorbers," NASA CR 120836, Jan. 1972.
- <sup>6</sup>Oberg, C. L., "Improved Design Techniques for Acoustic Liners," Rocketdyne, Canoga Park, Calif., Report No. RR-68-5, May 1968.
- <sup>7</sup>Oberg, C. L., Wong, T. L., and Schmeltzer, R. A., "Analysis of the Acoustic Behavior of the Baffled Combustion Chambers," NASA CR 72625, Jan. 1970.
- <sup>8</sup>Doak, P. E., "Excitation, Transmission and Radiation of Sound from Source Distributions in Hard-Walled Ducts of Finite Length (I): The Effects of Duct Cross-Section Geometry and Source Distribution Space-Time Pattern, (II): The Effect of Duct Length," *Journal of Sound and Vibration*, Vol. 31, Jan. 1973, pp. 1-72, and Feb. 1973, pp. 137-174.
- <sup>9</sup>Lansing, D. L. and Zorumski, W. E., "Effects of Wall Admittance Changes on Duct Transmission and Radiation of Sound," *Journal of Sound and Vibration*, Vol. 27, Jan. 1973, pp. 85-100.
- <sup>10</sup>Wynne, G. A. and Plumblee, H. E., "Calculation of Eigenvalues of the Finite Difference Equations Describing Sound Propagation in a Duct Carrying Shear Flow," presented at the 79th Meeting of the Acoustical Society of America, Atlantic City, N.J., April 21, 1970.
- <sup>11</sup>Baumeister, K. J., "Application of Finite Difference Techniques to Noise Propagation in Jet Engines," NASA TMX-68621, Nov. 1973.
- <sup>12</sup>Baumeister, K. J. and Rice, E. J., "A Difference Theory for Noise Propagation in an Acoustically Lined Duct with Mean Flow," *AIAA Progress in Astronautics and Aeronautics: Aeroacoustics: Jet*

and Combustion Noise, Vol. 37, Editor: Henry T. Nagamatsu; Associate Editors: Jack V. O'Keefe and Ira R. Schwartz, MIT Press, Cambridge, Mass., 1975, pp. 435-453.

<sup>13</sup>Alfredson, R. J., "A Note on the Use of the Finite Difference Method for Predicting Steady State Sound Fields," *Acustica*, Vol. 28, May 1973, 296-301.

<sup>14</sup>Cantin, G., "Three-Dimensional Finite Element Studies, Part One: Service Routines," Naval Postgraduate School, Monterey, Calif., NPS-59C 172121A, Dec. 1972.

<sup>15</sup>Chen, L. H. and Schweikert, D. G., "Sound Radiation from an Arbitrary Body," *Journal of the Acoustical Society of America*, Vol. 35, Oct. 1963, pp. 1626-1632.

<sup>16</sup>Chen, L. H., "A Matrix Method of Analysis of Structure-Fluid Interaction Problems," ASME Paper 61-WA-220, Aug. 1961.

<sup>17</sup>Chertock, G., "Sound from Vibrating Surfaces," *Journal of the Acoustical Society of America*, Vol. 36, July 1964, pp. 1305-1313.

<sup>18</sup>Copley, L. G., "Integral Equation Method for Radiation from Vibrating Bodies," *Journal of the Acoustical Society of America*, Vol. 42, April 1967, pp. 807-816.

<sup>19</sup>Banaugh, R. P. and Goldsmith, W., "Diffraction of Steady Acoustic Waves by Surfaces of Arbitrary Shape," *Journal of the Acoustical Society of America*, Vol. 35, Oct. 1963, pp. 1590-1601.

<sup>20</sup>Mitzner, K. M., "Numerical Solution for Transient Scattering from a Hard Surface of Arbitrary Shape-Retarded Potential Technique," *Journal of the Acoustical Society of America*, Vol. 42, Feb. 1967, pp. 391-397.

<sup>21</sup>Shaw, R. P., "Scattering of Plane Acoustic Pulses by an Infinite Plane with a General First-Order Boundary Condition," *Journal of Applied Mechanics*, Sept. 1967, pp. 770-772.

<sup>22</sup>Quinn, D. W., "An Integral Equation Method for Duct Acoustics with Varying Cross Sections and Axially Varying Impedance," *AIAA Journal*, Vol. 15, Feb. 1977, pp. 278-281.

<sup>23</sup>Liu, H. K. and Martenson, A. J., "Optimum Lining Configurations," *Basic Aerodynamic Noise Research*, NASA SP-207, July 1969, pp. 425-434.

<sup>24</sup>Zinn, B. T. and Gaylord, C. G., Unpublished Notes and "An Analytical Investigation of Acoustic Modes of Two and Three Dimensional Solid Rocket Motors," a Thesis Proposal by C. G. Gaylord, School of A. E., Georgia Tech., Atlanta, Ga.

<sup>25</sup>Tai, G. C. and Shaw, R. P., "Eigenvalues and Eigenmodes for the Homogeneous Helmholtz Equation for Arbitrary Domains," Report No. 90, Dept. of E. S., State University of N.Y. at Buffalo, Aug. 1973.

<sup>26</sup>Kellogg, O. D., Ch. VI, *Foundations of Potential Theory*, Dover Publications, New York, 1953.

<sup>27</sup>Webster, A. G., Ch. VIII, *The Dynamics of Particles*, Dover Publications, New York, 1959.

<sup>28</sup>Baker, B. B. and Copson, E. T., Ch. I, *The Mathematical Theory of Huygens' Principle*, Oxford at the Clarendon Press, 1950.

<sup>29</sup>Burton, A. J., "The Solution of Helmholtz's Equation in Exterior Domains Using Integral Equations," NPL Report NAC 30, National Physical Laboratory, Teddington, Middlesex, Jan. 1973.

<sup>30</sup>Strutt, J. W. (Lord Rayleigh), Ch. 16, *The Theory of Sound*, Vol. II, Dover Publications, New York, 1945.

<sup>31</sup>Ingard, K. U., "On the Theory and Design of Acoustic Resonators," *Journal of the Acoustical Society of America*, Vol. 25, Nov. 1953, pp. 1037-1061.

<sup>32</sup>Crocco, L. and Sirignano, W. A., "Behavior of Supercritical Nozzles under Three-Dimensional Oscillatory Conditions," AGARDograph 117, Butterworth Publications, London, 1967.

<sup>33</sup>Scott, R. A., "An Apparatus for Accurate Measurement of the Acoustic Impedance of Sound Absorbing Materials," *Proceedings of the Physical Society*, Vol. 58, 1946, p. 253.

<sup>34</sup>Zinn, B. T., Bell, W. A., and Daniel, B. R., "Experimental Determination of Three-Dimensional Liquid Nozzle Admittances," *AIAA Journal*, Vol. 11, March 1973, pp. 267-272.

<sup>35</sup>*T-Burner Manual*, Chemical Propulsion Information Agency, CPIA Publication No. 191, Nov. 1969.

<sup>36</sup>Crocco, L. and Cheng, S. I., "Theory of Combustion Instability in Liquid Propellant Rocket Motors," AGARDograph 8, Butterworth Publications, London, 1956.

<sup>37</sup>Culick, F. E. C., "Review of Calculations for Unsteady Burning of a Solid Propellant," *AIAA Journal*, Vol. 6, Dec. 1968, pp. 2241-2255.

<sup>38</sup>Conte, S. D., Chs. 2 and 5, *Elementary Numerical Analysis*, McGraw-Hill, St. Louis, 1965.

<sup>39</sup>Abramowitz, M. and Stegun, I. A., *Handbook of Mathematical Functions*, NBS AMS No. 55, May 1968.

<sup>40</sup>Bell, W. A., "Resonant Frequencies and Natural Modes of Arbitrarily Shaped Ducts," Final Report, NSF Research Initiation Grant GK-42159, Georgia Tech., Atlanta, Ga., April 1, 1976.

<sup>41</sup>Jones, D. S., "Integral Equations for the Exterior Acoustic Problem," *Quarterly Journal of Mechanics & Applied Mathematics*, Vol. 27, Jan. 1974, pp. 129-142.

<sup>42</sup>Greenspan, D. and Werner, P., "A Numerical Method for the Exterior Dirichlet Problem for the Reduced Wave Equation," *Archive for Rational Mechanics and Analysis*, Vol. 23, No. 4, 1966, pp. 288-316.

<sup>43</sup>Gradshteyn, I. S. and Ryzhik, I. M., *Table of Integrals, Series, and Products*, Sixth Printing, Academic Press, New York, 1972, 951.

<sup>44</sup>Hitchcock, A. J. M., "Polynomial Approximations to Bessel Functions of Order Zero and One and to Related Functions," *Math Tables & Other Aids to Computations*, Vol. 11, 1957, pp. 86-88.

<sup>45</sup>Bell, W. A., Meyer, W. L., and Zinn, B. T., "Prediction of the Acoustics of Solid Propellant Rocket Combustors by Integral Techniques," *Proceedings of the 12th JANNAF Meeting*, CPIA Publications No. 273, Vol. II, 1975, pp. 19-33.